Analysis of charge states in the mixed-valent ionic insulator AgO

Yundi Quan and Warren E. Pickett

Phys. Rev. B **91**, 035121 — Published 20 January 2015

DOI: 10.1103/PhysRevB.91.035121

Analysis of charge states in the mixed valent ionic insulator AgO

Yundi Quan and Warren E. Pickett
Department of Physics, University of California Davis, Davis, CA 95616
(Dated: December 3, 2014)

The doubly ionized d^9 copper ion provides, originally in La_2CuO_4 and later in many more compounds, the platform for high temperature superconductivity when it is forced toward higher levels of oxidation. The nearest chemical equivalent is Ag^{2+}, which is almost entirely avoided in nature. AgO is an illustrative example, being an unusual nonmagnetic insulating compound with an open $4d$ shell on one site. This compound has been interpreted in terms of one Ag^{3+} ion at the fourfold site and one Ag^{+} ion that is twofold coordinated. We analyze more aspects of this compound, finding that indeed the Ag^{3+} ion supports only four occupied $4d$-based Wannier functions per spin, while Ag^{+} supports five, yet their physical charges (as quantified by their spherical radial charge densities) are nearly equal. The oxygen $2p$ Wannier functions display two distinct types of behavior, one type of which includes conspicuous Ag $4d$ tails. Calculation of the Born effective charge tensor shows that the mean effective charges of the Ag ions differ by about a factor of two, roughly consistent with the assigned formal charges. We analyze the $4d$ charge density and discuss it in terms of recent insights into charge states of insulating (and usually magnetic) transition metal oxides. What might be expected in electron- and hole-doped AgO is discussed briefly.

PACS numbers: 71.28.+d, 75.20.Hr, 75.30.Mb

I. INTRODUCTION

Interest in understanding the charge state (or oxidation state, or formal valence) of transition metal cations in oxides and halides has recently resurfaced,[1–4] partly because it has been established that in many charge ordered systems discussed as being examples of disproportionation, the actual d electron occupation (i.e the charge) is invariant, to a high degree of accuracy.[1–4] There is interest also in obtaining an objective specification of the charge state of an ion,[2–4] since approaches that divide the total charge density amongst the various atoms[5,6] have not yet proven very useful. The rare earth nickelates have become one testing ground of models and theories, with a $2Ni^{3+} \rightarrow Ni^{2+} + Ni^{4+}$ disproportionation originally being envisioned to be responsible for the structural change and the accompanying metal-to-insulator transition. It has however become clear, at least for a few prominent examples,[1,4] that the signatures of "charge order" – the ionic radii, the magnetic moment, and splitting of core level energies – are obtained faithfully from density functional theory calculations in which there is no change in the actual charge ($4d$ occupation) of the Ni ion. The differences are due to the local environment: the available volume and the potential from neighboring oxygen ions, and the $4d-2p$ rebonding that will accompany a change in local environment.

There is interest in the doping of noble metal atoms to a valence higher than the common 1+ configuration of the closed shell ion, which occurs in typical band insulators. The 2+ state of noble metal atoms is of special interest, since the doping to higher levels for Cu, as from the La_2CuO_4 compound, leads the highest temperature superconductors (HTS) known, but with no increase in the superconducting critical temperature being achieved in the last twenty years. The square planar environment of the Cu^{2+} ion seems uniquely suited as the platform for HTS, but the underlying reasons are still under debate, making study of square planar Ag (and possibly Au) of obvious interest. Our goal is to quantify the difference between different charge states, and to do so in a variety of unusual systems so that some more general, and quantitative, recognition of differing charge states can be formulated and understood.

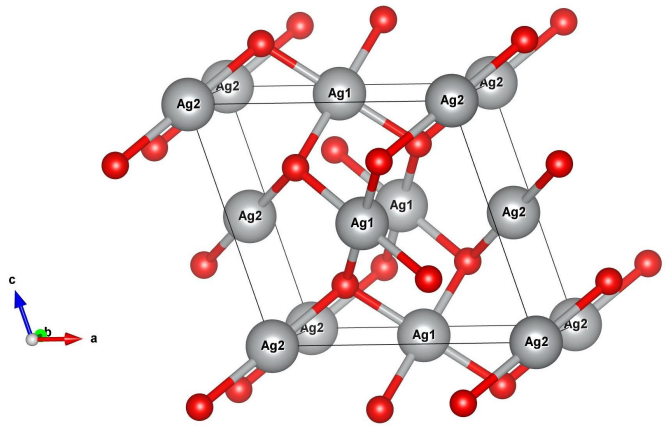

FIG. 1: Crystal structure of monoclinic AgO. Ag^{III} sits at the center of a slightly distorted but planar oxygen square, while Ag^{I} forms an O-Ag-O linear trimer with its nearest neighbors. Differences in coordination numbers and bond lengths suggest distinct charge states for Ag^{III} and Ag^{I}. The figure was produced using VESTA.[18]

A. Interest in the Ag cation

The two dimensional Ag^{2+} compound Cs_2AgF_4 provoked interest and study because it is isostructural with

the original cuprate superconductor La_2CuO_4 and contains a sister doubly charged noble metal ion, thereby raising hopes that it might also provide excellent superconductivity when doped. This compound, which also exists with other alkali cations, had been discovered[8,9] before superconductivity in the cuprates was found, and indeed the Ag ion is magnetic. The electronic structure is significantly different, however, and instead of being a high temperature antiferromagnet it is a low temperature ferromagnet – the magnetic coupling of Ag through fluorine is distinctly different from that of Cu through oxygen.[10] This compound thus became another example in the series of dashed hopes of finding a cuprate analog.

The unconventional insulating and nonmagnetic compound AgO presents related but distinct quandaries. The two Ag sites Ag1 and Ag2 consist of an O-Ag1-O linear trimer and an $Ag2O_4$ unit, in which this Ag ion is square planar coordinated (the unit is not precisely square). AgO has been characterized as mixed valent[11–13] Ag^{1+} and low-spin Ag^{3+} respectively, *i.e.* $Ag(I)Ag(III)O_2$. It should be emphasized that this difference is not a matter of disproportionation; the two sites are simply very different from the moment of crystallization. For transparency in nomenclature, in this paper we make the designation of the two Ag sites, and formal charges, explicit by using Ag^{III} and Ag^{I} rather than Ag1 and Ag2, respectively. We have shown elsewhere[4] that the two sites contain nearly the same amount of $4d$ charge, determined by the radial charge density in the vicinity of the $4d$ peak. The question is how to reconcile the apparent discrepancies – differing charge states with the same d charge – and more importantly how to understand differing charge states more generally in a microscopic manner.

The Ag ion is rather unusual. In the overwhelming number of compounds it is the simple closed shell ion Ag^{1+} $4d^{10}$. In a few systems it behaves differently. In $Ag_4(SO_3F)$ the Ag ion is suggested[14] to be mixed valent $2Ag^{1+}$ + Ag^{2+}, with two different sites as in AgO, surprising because Ag almost always avoids the divalent state. When it has no choice, as in AgF_2 with F being the most electronegative element, the magnetic $4d^9$ configuration emerges, and this compound becomes a canted antiferromagnet[15] below T_N=163K. A more exotic case arises in the double perovskite Cs_2KAgF_6 mentioned above, which remains cubic[16] because Ag acquires the high spin 3+ state which has cubic symmetry (e_g^2 spin-down holes).[17]

B. Investigation of formal valence

We have initiated a program of study of the charge state of cations in oxides (or halides, or nitrides) in relation to the physical charge and spin on the cation and the involvement of the environment, or more generally on the origin and identification of the formal valence of a transition metal based insulator. For several cases of "charge ordered" oxides, including $YNiO_3$, $CaFeO_3$, $AgNiO_2$, and V_4O_7, the different cation sites have the same $3d$ orbital occupation,[1,4] as seen from comparing the (spherically averaged) radial charge density $4\pi r^2\rho(r)$. From the two different charge state solutions obtained from density functional based calculations on La_2VCuO_6, the V^{4+} and V^{5+} ions have the same $3d$ occupation, and the Cu^{+} and Cu^{2+} ions also have the same occupation.[19] The difference lies in the distance from, and the degree and character of hybridization with, the neighboring shell of O ions.

Part of this program focuses on the objective identification of the charge state, or more generally the formal valence, of a cation M. The conventional method is to consider the average M-O distance, which provides an ionic radius, to consider the magnetic moment that gives the difference between occupations of up- and down-spins, and to impose charge neutrality. From theoretical calculations, one analyzes band characters to identify the number of primarily M orbitals and the difference between the up and down occupations, and decides on the charge state, always respecting charge neutrality. In a large majority of cases there is little if any ambiguity. There are a growing number of cases, however, in which the assigned formal valences don't seem to provide a viable characterization. Experimentalists have, for example, fit data on disproportionated $YNiO_3$ and characterized the ions[20] as $Ni^{(3\pm\delta)-}$ with $\delta \approx 0.3$, which is at best an extrapolation of the concept of formal valence. Several reasons why a conventional charge-order picture of the structural and metal-insulator transition in $YNiO_3$ does not hold up have been presented earlier.[1]

Returning to the issue of the charge ascribed to a particular ion and recognizing that actual occupations should not be expected to be integers (nor even close), there have been proposals of how to apportion charge between atoms or ions. The early quantum-chemistry-based Mulliken decomposition of the charge of neighboring atoms is somewhat arbitrary and has been found to be too strongly dependent on the basis set of atomic orbitals that is used. The 'generalized pseudoatom' decomposition of charge proposed by Ball,[21] and later made more specific as 'enatom,'[5] appears to be inappropriate for quantitative study of insulators. The decomposition given by Bader[6,39,40] has not yet been applied very widely to transition metal insulators. Values that have been reported:

- for nickelates,[4] +1.33 and +1.49 for the two Ni sites in $YNiO_3$, +1.15 and +1.20 for the two Ni sites in $AgNiO_2$;
- for the ferrite $CaFeO_3$, +2.03 and +1.99 for the nominal Fe^{3+} and Fe^{5+} ions;[7]
- for Ag oxides, around +1.1 and +0.6 for the two sites in AgO,[4,22], +0.52 for Ag in Ag_2O,[22], +1.23 for Ag in Ag_2O_3.[22]

Without additional knowledge, these values would not necessarily suggest specific charge states. Note that in $YNiO_3$, $AgNiO_2$, and AgO the formal valences would differ by two, whereas the Bader charges differ by only a few tenths of the fundamental electron charge. In these

systems the Bader charge of oxygen is typically -0.8 to -1.0.

Two proposals have arisen lately as potentially objective means of identifying charge states, also based on the charge density. Sit *et al.*[2] proposed using the orbital occupation values that arise already in carrying out correlated density functional calculations (see the next section) to identify *occupied* and *unoccupied* orbitals, which then determines the charge state. For distorted $AgNiO_2$, it was found[4] that this prescription works (only) if 94% is identified as filled while 68% qualifies as unfilled. More borderline cases might also arise. Separately, Jiang *et al.*[3] showed that, if one can distort the structure to translate the cation sublattice through one primitive lattice vector while preserving an insulating state, an integer "charge" arises as in integrated polarization that would be natural to identify with the charge state of the ion. This proposal suffers from the likelihood that the resulting charge can depend on the direction of displacement, much as the Born effective charge can be anisotropic and thus unsuitable, *inter alia*, as a scalar charge state. More applications of this procedure will be useful in clarifying the utility of this approach.

As part of a general effort to understand better the *charge states* in strongly ionic materials and more generally the *formal valence* in insulators, we are pursuing a specific proposition: can the charge state of cations in oxides, halides, and nitrides be identified from the number of Wannier functions of each spin that can be assigned to specific cation? First, if maximally localized Wannier functions are used, the answer is unique in principal, with possible challenges in finding the truly most localized set. Importantly, as long as assignments to specific atoms can be made objectively, the result is an integer. Finally, separation of the (valence) charge into MLWFs comprises a unique separation of the full charge density into individual one-unit-charge entities, and provides the opportunity to analyze how the separation differs for differing charge states of a given ion.

C. Plan of this paper

In this paper, we focus on charge state characterization of the charge states of Ag^{III} and Ag^{I} sites in AgO by using various methods including Born effective charge, real space charge density and Wannier function analysis. We demonstrate for this unusual case that the charge state picture bears no relation to the static charge distribution, instead simply reflecting the local environment including the distance of negative ions and the resulting $d-p$ bonding. Nevertheless, the formal charge provides a physical description that has important consequences for the understanding of the observed properties of this compound.

While the Ag^{III} site has sometimes been characterized as Ag^{II} plus oxygen holes, this compound is not a very ambiguous case. A well known system that is not so clear-cut is that of the "charge-ordering" rare earth nickelates. Our earlier work[1] pointed out that there is no difference in $3d$ occupation between the supposed Ni^{2+} and Ni^{4+} sites, the latter of which had been strongly argued to be Ni^{2+} plus oxygen holes. The most studied member, $YNiO_3$, had been characterized by fitting experimental data as $Ni^{3\pm\delta}$ with $\delta \approx 0.3$ (see Quan *et al,*[1] for more discussion and references). For $YNiO_3$ the Wannier function analysis has been applied[4] to justify the *formal* designations as Ni^{2+} and Ni^{4+} in spite of any meaningful difference in $3d$ occupations of the Ni ions.

II. STRUCTURE AND METHODS

The space group of crystalline AgO is monoclinic $P2_1/c$ (#14), with two non-equivalent Ag sites (Ag^{III}, Ag^{I}) but a single oxygen site, $2d$, $2a$ and $4e$ respectively. Ag^{III} sits at the center of a planar, slightly distorted oxygen square, with bond lengths 2.03 Å and 2.02 Å, while Ag^{I} and its nearest neighbor oxygens form a linear trimer with bond length 2.16 Å. There is a single O site and each oxygen is shared by two squares and one trimer. Since the Ag^{I}-O bond is 0.13 Å longer than the Ag^{III}-O bond, and the Ag^{III} coordination number is twice that of Ag^{I}, the charge state of Ag^{III} and Ag^{I} have been characterized as 3+ and 1+ to balance $2O^{2-}$. The corresponding $4d$ occupation of Ag^{III} and Ag^{I} are (low spin) (S=0) $4d^8$ and closed shell $4d^{10}$ respectively, in agreement with insulating diamagnetism of AgO.

We have carried out density functional theory DFT calculations using the linearized augmented plane wave method as implemented in WIEN2k.[23] The local density approximation (LDA) exchange-correlation functional of Perdew and Wang[24] was used. Because Ag^{III} is an open-shell ion, we applied the LDA+U method to probe correlation effects beyond LDA, in spite of the low-spin (non-magnetic) state of the ion. U was increased from 0.1Ry with both the "around mean field" (AMF) and "fully localized limit" (FLL) double-counting functionals.[25] In both cases, the band gap increases slowly and almost linearly with increasing U, by around 50 meV per 1 eV increase in U, thus a U value of 4 eV (perhaps an upper limit) still leaves a severe underestimate of the observed gap.

In recent years Wannier functions, which are localized orbitals obtained as lattice Fourier transforms of linear combinations of Bloch states, have become an indispensable tool in analyzing properties of crystalline insulators. The indeterminacy of the arbitrary phases involved in mixing the Bloch functions, and consequently the unitary transformation matrix, leads to extra degrees of freedom which can be eliminated by imposing certain conditions (choosing gauges). In this paper, we use maximally localized Wannier functions (WFs) which are obtained by minimizing the spread functional.[26,27] The overlap matrix calculation and post-processing were carried out with *wien2wannier*[28] code. For the spread functional mini-

mization, we used Wannier90,[29] which is independent of the basis functions used in DFT calculations.

We have found some results are sensitive to k-point sampling, no doubt because of the small gap which can lead to changing orbital character as bands approach each other and hybridization evolves. We have used 14 by 22 by 15 k-mesh in the zone for the LDA+U and TB-mBJ calculations, and 10 by 16 by 11 k-mesh for the Wannier functions to achieve good convergence.

III. RESULTS

A. Previous work

A few theoretical studies of AgO using first principle method have been reported. Park *et al*[30] addressed the difference between Ag^{III} and Ag^{I} by analyzing partial densities of states (PDOS). They demonstrated that Ag^{I} has significant spectral weight and strong hybridization with oxygen only in the region below the Fermi level, while there exists a Ag^{III} d peak immediately above the Fermi level which is equally strongly hybridized with oxygen. At the experimental geometry, LDA and GGA give an almost exactly vanishing gap (using a 5000 point k-mesh for self-consistency). Recent work by Allen *et al.* using pseudopotential methods with a hybrid functional (part Hartree-Fock exchange, part local density exchange) calculation gives a direct band gap of 1.2eV[22,32] which is consistent with the optical band gap of 1-1.1eV observed from experiment.[31]

Further discussion of the $4d-2p$ hybridized contour and PDOS was provided by Pickett *et al.*,[4] including a plot of the charge density displaying all ions from the unoccupied "$Ag^{III}O_4$" band, which contains significant Ag^{I} character as well. These authors also noted that there is negligible difference in $4d$ occupation on the two Ag sites – the spherically averaged charge densities in the vicinity of the $4d$ peak are the same – and that the orbital occupations of the two sites strains the rule proposed by Sit *et al.*[2] that formal charges of ions can be obtained from orbital occupations that are used in LDA+U calculations.

For orientation the atom-projected density of states (PDOS) is presented in Fig. 2. These results are not for LDA or GGA, however, which as mentioned above give a very small gap.[22] These PDOSs are the result of applying (i) the LDA+U method with U=4 eV, J = 0.68 eV, and (ii) the modified Becke-Johnson (mBJ) potential, which is known to greatly improve on the gaps of a few classes of insulators, compared to the LDA or GGA result. The form we have used is the Tran and Blaha modification[34,35] TB-mBJ. It incorporates the orbital kinetic energy density into the potential as a improved way[36,37] of representing the non-local exchange potential, with little expense beyond reconverging to self-consistency. For AgO, the mBJ potential leads to a gap of 0.4 eV.

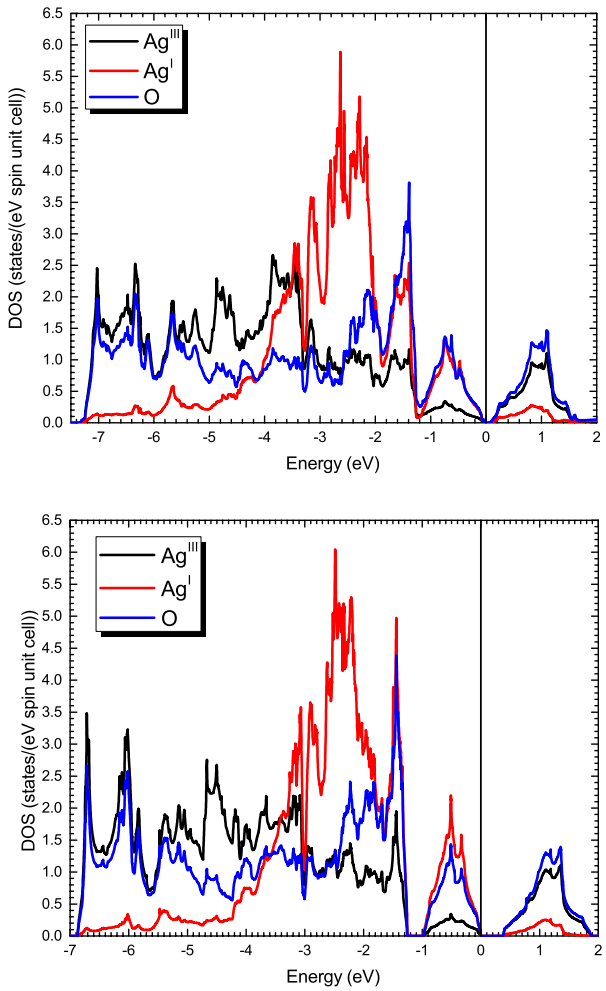

FIG. 2: Atom-projected density of states of AgO. Above: LDA+U calculation with around mean field (AMF) double counting. Below: TB-mBJ potential calculation as described in the text. The bottom of the gap is taken as the zero of energy. In both cases the Ag^{III} DOS extends to low energy (-7 eV) as well as dominating over Ag^{I} in the unoccupied band around 1 eV. The differences are the size of the gap – larger for TB-mBJ – and the width of the highest occupied band, which is 20% narrower for the TB-mBJ case.

Fig. 2 illustrates the very different spectral distributions of the Ag^{III} and Ag^{I} $4d$ states. The former has weight distributed throughout the -7 eV to -1 eV region, whereas the latter has its weight concentrated in only the upper half of this range – its states are much less strongly bound. In the 1 eV range below the valence band maximum, there is one band per Ag pair per spin that has a majority of Ag^{I} weight, however it has substantial $AgIII$ weight as well. Above the gap is one more band per Ag pair per spin that is heavily Ag^{III} hybridized with O $2p$, and very little Ag^{I} weight; this band has been identified as the unoccupied band of the $4d$ ion.[30]

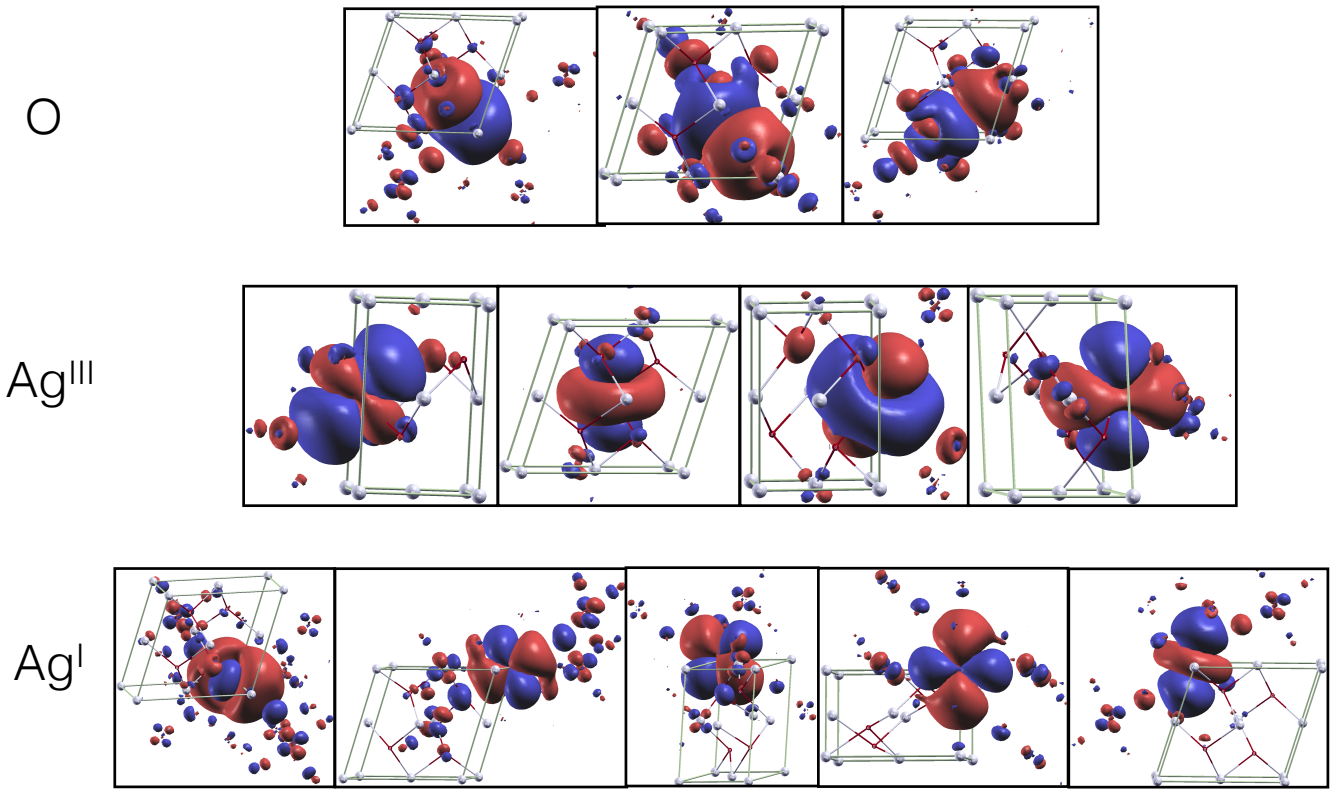

FIG. 3: Isosurface plots of the Ag $4d$ maximally localized Wannier functions of AgO, red and blue denote opposite signs. The top three are O-centered, $2p$-based; note that the latter two have substantial contributions from an Ag orbital only at one end. The next four are centered at Ag^{III} d^8 site and are more confined but larger on the Ag site, while the bottom five are centered at the Ag^I d^{10} site. Each of the four Ag^{III} WFs contains more $4d$ charge than does an Ag^I WF, but the latter WFs include more neighboring O $2p$ contribution. All isosurface values are the same. These WFs were obtained from a $10\times16\times11$ Brillouin zone mesh.

B. Wannier function analysis of AgO

The formal charge states correspond to four occupied orbitals per spin for Ag^{III}, five for Ag^I, and of course three for each O^{2-}. The manifold of bands used for $Ag^I Ag^{III} O_2$ in the WF calculation consists of 30 isolated valence bands immediately below the gap, which are Ag $4d$ bands mixed with oxygen $2p$ bands. The spread functional minimization leads to localized site-centered $4d$-derived WFs at Ag^{III} and Ag^I sites, and Wannier functions at the O sites that, notably, are not exactly site centered.

Isosurfaces of the WFs for AgO are plotted in Fig. 3. We obtain four WFs centered at Ag^{III} site and five centered on Ag^I. The WFs at the Ag^I site, shown in Fig. 3, have at their core the classic shape of the five d orbitals. Their orientation is non-intuitive, moreover their extension includes neighboring O $2p$ contributions and even neighboring Ag $4d$ contributions. The four WFs at the Ag^{III} site have a core that is of $4d$ shape as well. However, one of the five $4d$ orbitals is missing; on the other hand, the volumes at the chosen isosurface are larger than for the Ag^I WFs, that is, the unit charge of these WFs contain more contribution from the $4d$ orbitals than do the WFs centered on Ag^I. This characteristic provides some of realities of hybridization that have been used by a few to consider the Ag^{III} site to be better characterized as Ag(2+) plus oxygen holes.

While the WFs of Ag are centered on the nuclear sites, the centers of the O WFs differ from oxygen nuclear positions, by values of 0.13 Åand 0.33 Å(twice). These displacements reflect first, polarization of the O^{2-} ions that is non-intuitive due to its low site symmetry, and secondly, the substantial admixture of Ag contributions to two of them. In the figure, it can be seen that of the three O $2p$ WFs, one has exemplary O $2p$ character while the other two represent O $2p$ orbitals that are strongly mixed with an Ag^{III} $4d$ orbital - one $4d$ tail extends from each of two O $2p$ WFs. The mixing of Ag^{III} $4d$ orbital to the oxygen $2p$ WF is aligned along the diagonal of the oxygen plaquette. Consequently, the Wannier functions for oxygens sitting at opposite ends of the diagonal have significant overlap.

To assess the $4d$ charge distributions, the decomposed radial charge densities inside Ag^{III} and Ag^I spheres are displayed in Fig. 4. The black and red lines are the decomposed radial charge densities of WFs in the Ag^{III}

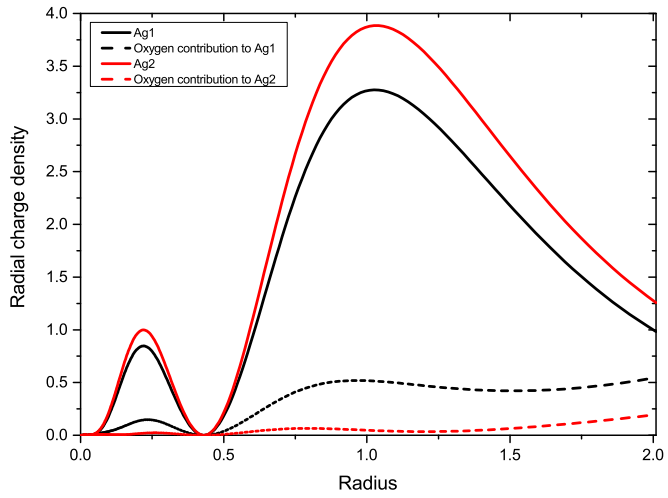

FIG. 4: Black solid line: radial charge densities $4\pi r^2\rho(r)$ versus distance from the Ag nucleus, in a.u. Red solid line: sum from the five Ag^I WFs. Black solid line: sum from four Ag^{III} WFs. Dashed lines: corresponding contributions from the O $2p$ WFs within the Ag spheres.The O WFs make large contributions to the Ag^{III} atomic density.

and Ag^I spheres respectively. Solid lines are the contribution from $4d$ WFs (and their translated images); dashed lines are the contribution from oxygen-based WFs. The lower contribution to the $4d$ occupation from four WFs of Ag^{III}, versus five for Ag^I, are almost exactly compensated by the contribution from the two of the O-centered WFs. The resulting equivalence of real charge on ions characterized by different charge states has become a recurring theme in magnetic "charge-ordered" compounds, thus comes over to nonmagnetic AgO.[1,4]

The charge differences can be quantified in another way; the Ag^1 site always has slightly more charge. Integrating charge to the peak in the $4d$ radial charge density at 1.01 a.u., the difference is 0.02 e. Integrating to 1.5 a.u., the difference is 0.11 e, and at 2.0 a.u. the difference is decreased to 0.08 e each including both spins. Thus while this difference is small, it is in a different class from the other two charge state systems we have studied,[4] where differences were 0.02 e or less.

C. Comments on energies

WFs provide an orthonormal tight-binding representation of the band structure in the region spanned by the WFs. Characteristics of interest include the on-site energies and hopping amplitudes, the latter of which for nine Ag WFs and six O WFs are too numerous to present. For these maximally localized WFs, we find the interactions are mostly short-range. The band structure obtained from diagonalizing the Hamiltonian with truncated summation (after few neighboring cells) agrees well with the band structure from DFT calculation.

The onsite energies of all occupied WFs are listed in Table I. Ag^{III} on-site energies range from -4.49eV to -3.94eV, with one split off from the rest by 0.5 eV. The Ag^I on-site energies range from -2.86eV to -2.59eV, a rather small range for transition metal ions in oxides. The oxygen on-site energies are more interesting, ranging over nearly 1 eV, with a pair at -4.30±0.03 eV and the other at -3.42eV. As mentioned above, two of the oxygen WFs have substantial Ag $4d$ tails inside Ag^{III} sphere, and the on-site energies reflect this distinction. Hopping parameters between oxygen Wannier functions that extend into a given Ag^{III} site are as large as -1.0 eV, reflecting the strong interaction between neighboring O orbitals through Ag^{III} orbitals.

The fifth Ag^{III} WF would correspond to the unoccupied band just above E_F. Due to the band crossing with a higher lying band, there is entanglement with conduction band WFs and we have not obtained this WF. Its site energy presumably would lie much nearer to, if not above, the bottom of the gap. Note also that there is not a distinct Ag^I-derived WF corresponding to the $4d$ band 0.5 eV below E_F; all of the Ag^I WFs have site energies around -2.7 eV.

Atom	on-site energies					mean
Ag^{III}	-3.94	-4.49	-4.44	-4.31	—	-4.29
Ag^I	-2.59	-2.73	-2.82	-2.86	-2.78	-2.76
O	-3.42	-4.27	-4.33	—	—	-4.00

TABLE I: On-site energies (eV) of the occupied Wannier functions described in the text and shown in Fig. 3. Note that for Ag^{III} and for O one site energy is separated substantially from the others, while there is little crystal field splitting for Ag^I. Since the GGA gap is vanishingly small (slightly negative), these site energies were checked up to a 14×22×15 Brillouin zone integration mesh.

D. Born Effective Charge of AgO

The Born effective charge (BEC) tensor $Z_{\alpha\beta}$ is a measure of the dynamic response of electron system to ionic displacements. Vibrating ions drive electric response as if they had this charge. Using the finite displacement method, we calculated the BECs of Ag^{III}, Ag^I and O in Cartesian coordinates. The displacements Δx_j along $\vec{a}$, $\vec{b}$ and $\vec{c}$ were 0.001 in internal units, within the linear response regime. Since the lattice vectors of AgO are non-orthogonal, we chose to have $\hat{y}$ and $\hat{z}$ pointing along $\vec{b}$ and $\vec{c}$ respectively. In the Cartesian coordinate system, the change in polarization ΔP is related to displacements Δx_j by

$$\Delta P_i = \frac{e}{\Omega}\sum_{j=x,y,z} Z_{ji}\Delta x_j \qquad (i=x,y,z) \qquad (1)$$

where Ω is the cell volume. Eighteen separate calculations were carried out displacing Ag^{III}, Ag^I and O along

Ag^{III}			Ag^{I}			O		
0.83	-0.96	0.58	1.49	0.34	0.06	-1.15	0.10	-0.33
-0.20	2.16	-1.20	0.32	0.72	0.49	0.15	-1.43	1.11
-0.27	0.34	3.58	-0.14	-0.16	1.12	0.19	0.82	-2.35
$2.94 \pm 0.41i$		0.69	1.51	1.13	0.69	-2.93	-1.11	-0.89

TABLE II: The Born effective charge tensors for Ag^{III}, Ag^{I} and O. The eigenvalues are provided on the bottom line.

$\vec{a}$, $\vec{b}$ and $\vec{c}$ respectively. Polarization was calculated using the BerryPi code.[38] We used the LSDA+U method with U=4.08 eV, J=0.68 eV. We obtained the Born effective charge tensors for Ag^{III}, Ag^{I} and O, shown in Table 2.

The unusual open shell but low spins Ag^{III} ion has complex eigenvalues of the BEC tensor. We confirm that $\sum_s Z_{s,\alpha\alpha} = 0$ ($\alpha = x, y, z$) as required by the acoustic sum rule. Eigenvalues (see Table II) of Z_{Ag^I} are in rough agreement with a 1+ formal charge state characterization. Eigenvalues of Z_O, -2.93, -1.11 and -0.89, are highly direction dependent. The modulus of the complex eigenvalues (complex conjugates) of Ag^{III} is 2.97, which is close to its formal valence.

IV. COMMENTS ON DOPING

Extrapolating from the doping of Cu^{2+} states that are square coordinated with oxygen and lead to high temperature superconductivity, possible effects of doping of AgO become of interest. Typical samples of AgO are slightly doped n-type,[13] such as might arise from oxygen vacancies, and thin Ag-O films that are transparent conductors are believed to involve AgO. The 1 eV bandwidths of both the highest occupied band and the lowest unoccupied band (see Fig. 2), together with the nearly 100% underestimate of the gap by the local density approximation, suggests that correlation effects will be important for the doped carriers, which might arise from either Coulomb interactions or electron-lattice interaction.

A guide to what can be expected can be obtained from the PDOS shown in Fig. 2. Excess electrons will inhabit the empty Ag^{III} band, where mixing with O $2p$ is very strong. The relevant orbital is the corresponding $Ag^{III}O_4$ cluster orbital (Wannier function). Strong electron-lattice coupling may result in polaronic conduction or, at low doping, localization. The carriers are likely to be magnetic on a time scale that could lead to a large susceptibility per carrier.

The small bandwidth and strong interaction aspects should apply to hole doping as well. A qualitative difference is that holes enter $4d$ states on the two-fold coordinated Ag^{I} ion. Hopping to neighboring Ag^{I} sites are strongly inhibited however, because each O ion is linked to two square units but only a single trimer. A hole on a trimer must tunnel through a square to reach another trimer, in order to move through the lattice. Thus there will be a much stronger tendency for holes to localize and also to be magnetic, than for electrons. This picture is consistent with conductivity in AgO being n-type.

Much the same behavior can be seen in lightly hole-doped cuprates, where antiferromagnetic order (or strong correlations) also contribute. Approximately 5% holes must be doped in, only then does the system become conducting and superconducting. There are of course several differences besides the magnetism between the AgO compound studied here and the cuprates: two dimensional layers, relatively straightforward hopping of carriers, and several others. The similarities do seem intriguing enough that doping studies of AgO should be pursued.

V. SUMMARY

In this paper we have studied the electronic structure, the ionic character, and the dynamic linear response of the system to ionic displacements. Specifically, we have analyzed the character of the two very distinct Ag sites focusing on a "charge state" (formal oxidation state) picture. As we have found in several related "charge disproportionated" materials,[4] the $4d$ occupations of the two Ag ions are nearly the same, based on the magnitude of the Ag radial charge density in the vicinity of the $4d$ peak. On the other hand, maximally localized Wannier functions are calculated, finding that there are four $4d$-like Wannier functions per spin centered on Ag^{III} while there are five $4d$-like Wannier functions per spin on Ag^{I}. This distinction, as well as the computed Born effective charges, are in agreement with the 3+ and 1+ characterization of the charge states.

The characters of the WFs at the two sites are different: the Ag^{I} WFs include larger contributions from neighboring oxygens, with noticeable contribution from neighboring Ag sites as well. Additionally, the average on-site energies differ by 1.5 eV. The three O WFs also display two types of behavior: two have strong admixtures with Ag^{III} d orbitals, while the other is of the more classic type of nearly pure oxygen $2p$ orbital. The two similar WFs differ in site energy by almost 1 eV from the third. Only when contributions from all Ag and O WFs are included do the charge densities on sites Ag^{III} and Ag^{I} become nearly the same.

The Born effective charge tensors reflect the low site symmetries of the ions, and reveal very strong directional dependence. For Ag^{III}, the maximum diagonal element is 3.6, very consistent with a 3+ designation. The minimum element is however only 23% of that. For Ag^{I}, the values range over a factor of two. Still, the rms values of the moduli of the tensor eigenvalues differ by a factor of two, indicating large differences consistent with very different formal valences. Overall, our calculations support (1) the longstanding view that the two Ag sites merit 1+ and 3+ designations, and (2) our recent suggestion[4] that it is the number of occupied Wannier functions that correlates with its charge state. This work has revealed that

the differences in the character of the Wannier functions for the two charge states can be substantial.

VI. ACKNOWLEDGMENTS

The authors would like to thank Elias Assmann for providing useful discussion about the wien2wannier code, Oleg Rubel for providing BerryPi code, and many useful discussions with Antia S. Botana. This work was supported by Department of Energy grant DE-FG02-04ER46111.

[1] Y. Quan, V. Pardo, and W. E. Pickett, Phys. Rev. Lett. **109**, 216401 (2012).
[2] P. H.-L. Sit, R. Car, M. H. Cohen, and A. Selloni, Inorg. Chem. **50**, 10259 (2011).
[3] L. Jiang, S. V. Levchenko, and A. M. Rappe, Phys. Rev. Lett. **108**, 166403 (2012).
[4] W. E. Pickett, Y. Quan, and V. Pardo, J. Phys.: Condens. Matter **26**, 274203 (2014).
[5] J. Kunstmann, L. Boeri, and W. E. Pickett, Phys. Rev. B **75**, 075107 (2007).
[6] R. F. W. Bader, *Atoms in Molecules: a Quantum Theory* (Oxford University Press, New York, 1990).
[7] Y. Wang, S. H. Lee, L. A. Zhang, S. L. Shang, L.-Q. Chen, A. Derecskei-Kovacs, and Z.-K. Liu, Chem. Phys. Lett. **607**, 81 (2014).
[8] R. Hoppe, Angew. Chem. Int. Ed. Engl. **20**, 63 (1981).
[9] W. Grochala and R. Hoffmann, Angew. Chem. Intl. Ed. **40**, 2742 (2001).
[10] D. Kasinathan, K. Koepernik, U. Nitzsche, and H. Rosner, Phys. Rev. Lett. **99**, 247210 (2007).
[11] K. Yvon, A. Bezinge, P. Tissot, and P. Fisher, J. Solid State Chem. **65** 225-230 (1986).
[12] P. Tissot, Polyhedron **6**, 1309 (1987).
[13] M. Bielmann, P. Schwaller, P. Ruffieux, O. Gröning, L. Schlapbach, and P. Gröning, Phys. Rev. B **65** 235431 (2002).
[14] T. Michalowski, P. J. Malinowski, M. Derzsi, Z. Mazej, Z. Jagličić. P. J. Leszczyński, and W. Grochala, Eur. J. Inorg. Chem. **2011**, 2508 (2011).
[15] P. Fischer, G. Roult, and D. Schwarzenbach, J. Phys. Chem. Solids **32**, 1641 (1971).
[16] R. Hoppe and R. Hoffmann, Naturwissenschaften **53**, 501 (1966).
[17] T. Jia, X. Zhang, T. Liu, F. Fan, Z. Zeng, X. G. Li, D. I. Khomskii, and H. Wu, Phys. Rev. B **89**, 245117 (2014).
[18] K. Momma and F. Izumi, "VESTA 3 for three-dimensional visualization of crystal, volumetric and morphology data," J. Appl. Crystallogr. **44**, 1272-1276 (2011).
[19] V. Pardo and W. E. Pickett, Phys. Rev. B **84**, 115134 (2011).
[20] U. Staub, G. I. Meijer, F. Fauth, R. Allenspach, J. G. Bednorz, J. Karpinski, S. M. Kazakov, L. Paolasini, and F. d'Acapito, Phys. Rev. Lett. **88**, 126402 (2002).
[21] M. A. Ball, J. Phys. C **10**, 4921 (1977) and references therein.
[22] J. P. Allen, D. O. Scanlon, and G. W. Watson, Phys. Rev. B **81**, 161103(R) (2010).
[23] P. Blaha, K. Schwarz, G. K. H. Madsen, D. Kvasnicka, and J. Luitz, WIEN2k, An Augmented Plan Wave+Local Orbitals Program for Calculating Crystal Properties (Karlheinz Schwarz, Techn. Universität Wien, Austria, 2001), ISBN 3-9501031-1-2
[24] J. P. Perdew and Y. Wang, Phys. Rev. B **45**, 13244 (1992).
[25] E. R. Ylvisaker, W. E. Pickett and K. Koepernik Phys. Rev. B **79**, 035103 (2009).
[26] N. Marzari, A. A. Mostofi, J. R. Yates, I. Souza, and D. Vanderbilt, Rev. Mod. Phys. **84**, 1419 (2012).
[27] N. Marzari and D. Vanderbilt, Phys. Rev. B **56**, 12847 (1997).
[28] J. Kunes, R. Arita, P. Wissgott, A. Toschi, H. Ikeda, K. Held, Comp. Phys. Commun. **181**, 1888 (2010).
[29] A. A. Mostofi, J. R. Yates, Y.-S. Lee, I. Souza, D. Vanderbilt, and N. Marzari, Comput. Phys. Commun. **178**, 685 (2008).
[30] K.-T. Park, D. L. Novikov, V. A. Gubanov, and A. J. Freeman, Phys. Rev. B **49**, 4425 (1994).
[31] N. R. C. Raju, K. J. Kumar, and A. Subrahmanian, J. Phys. D: Appl. Phys. **42**, 13 (2009).
[32] J. P. Allen, D. O. Scanlon, and G. W. Watson, Phys. Rev. B **84**, 115141 (2011).
[33] C. Brouder, G. Panati, M. Calandra, C. Mourougane, and N. Marzari, Phys. Rev. Lett. **98**, 046402 (2007).
[34] F. Tran and P. Blaha, Phys. Rev. Lett. **102**, 226401 (2009).
[35] A. D. Becke and E. R. Johnson, J. Chem. Phys. **124**, 221101 (2006).
[36] R. T. Sharp and G. K. Horton, Phys. Rev. **90**, 317 (1953).
[37] J. D. Talman and W. F. Shadwick, Phys. Rev. A **14**, 36 (1976).
[38] S. J. Ahmed, J. Kivinen, B. Zaporzan, L. Curiel, S. Pichardo, and A. Rubel, Comput. Phys. Commun. **184**, 647 (2013).
[39] A. Otero-de-la-Roza, E. R. Johnson and V. Luaa, Comput. Phys. Commun. 185, 10071018 (2014)
[40] A. Otero-de-la-Roza, M. A. Blanco, A. Martn Pends and V. Luaa, Comput. Phys. Commun. 180, 157166 (2009)